Quality Assessment of Finger-vein Image

Huafeng Qin[1, 2]*, Sheng Li[2], Alex C. Kot[2], and Lan Qin[1]
[1] College of Opto-Electronic Engineering, Chongqing University, Chongqing 400030, PR. China.
Email: N1107450K@ntu.edu.sg, qinlan@cqu.edu.cn
[2] School of Electrical and Electronic Engineering, Nanyang Technological University, Singapore 640732, Singapore.
Email: (Lish0016, eackot)@ntu.edu.sg

Abstract—**In this paper, we propose a novel quality assessment of finger-vein images for quality control purpose. First of all, we divide a finger vein image into a set of non-overlapping blocks. In order to detect the local vein patterns, each block is projected into the Radon space using an average Radon transform. A local quality score is estimated for each block according to the curvature in the corresponding Radon space, based on which a global quality score of the finger-vein is computed and assessed. Experimental results show that our approach can effectively identify the low quality finger-vein images, which is also helpful in improving the performance of a finger-vein recognition system.**

***Keywords*—finger-vein image, quality assessment, Radon transform**

I. INTRODUCTION

Biometrics authentication is a method of recognizing a person based on his physiological or behavioral characteristic such as fingerprint, finger-vein, face and signature. Compared with traditional authentication techniques based on passwords, the biometric techniques are more convenient and secure. Therefore, biometric techniques are widely used in authentication systems nowadays.

Among all the biometric techniques, most of the extrinsic biometric traits (e.g., fingerprint and face) are susceptible to spoof attacks on the sensor level. For example, an attacker can manufacture a fake finger according to a stolen fingerprint template. By scanning the fake finger, the attacker may be able to break into some fingerprint recognition systems which store the original fingerprint. On the contrast, the intrinsic biometrics traits (eg., finger-vein [1-3] and palm-vein [4]) are beneath the surface of the human body, which are more difficult to be forged [4]. Among the intrinsic traits, capturing finger-vein is very convenient, which can be easily adopted in various applications.

In a finger-vein recognition system, the finger-vein image acquisition process is affected by many factors such as environmental illumination [3], ambient temperature [1], [2], physiological changes [1], [2] and user behavior [3]. If these factors are not well established, the quality of the captured finger-vein image will be poor, which will eventually affect the performance of the system. Therefore, it is necessary to measure the quality of the finger-vein image before it is processed for matching.

In recent years, various quality assessment approaches have been proposed for different biometric traits. For example, the works in [5] propose several approaches for measuring the quality of the fingerprint images. By incorporating these approaches, the system designer is able to control the quality of the fingerprint images for the enrollment and query, so as to increase the performance of the fingerprint recognition systems. For the same purpose, quality assessment approaches are proposed for face [6] and iris [7]. However, to the best of our knowledge, there is no existing technique designed specifically for measuring the quality of the finger-vein images.

From the user point of view, the low quality finger-vein images are mainly created due to inappropriate behaviors during the image acquisition process including:

1) Incorrect placement of the finger: the location of the finger is incorrect on the capturing device. The near infrared light will be irradiated on the boundary of the finger or directly on the finger slot, which can heavily degrade the contrast of the vein patterns or even break the vein patterns in the finger-vein image as shown in Fig. 1(a).

2) High pressure or forcefully stretch of the finger: the finger is strongly pressed on the finger slot or forcefully stretched. The high pressure or stretch makes the vein pattern unclear or even disappeared in the finger-vein image as shown in Fig. 1(b).

3) Movement of the finger: the finger is moved during the capturing process. The movement will also create a finger-vein image with vein patterns of a low contrast as shown in Fig. 1(c).

Based on the above observations, a novel approach for finger-vein image quality assessment is proposed in this paper, which focuses on measuring the quantity and contrast of the vein patterns in a finger-vein image. Specifically, each block of a finger-vein image is projected into the Radon space using an average Radon transform. Local quality scores are estimated based on the curvatures of the blocks in the Radon space, from which a global quality score is computed for the finger-vein image.

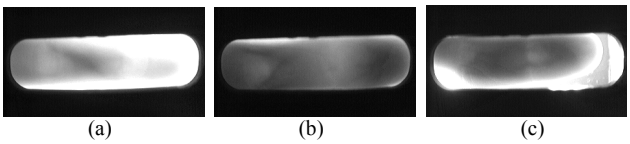

(a) (b) (c)

Fig.1. Low quality finger-vein images created due to inappropriate user behaviors: (a) incorrect placement of the finger, (b) high pressure or forcefully stretch of the finger and (c) movement of the finger.

By using our quality assessment approach, if the user's behavior is not appropriate during the image acquisition process, a low quality score may be assessed to the captured finger-vein image, which will be rejected before the finger-vein matching. The experimental results show that our approach works well for identifying the low quality finger-vein images. It is also useful for improving the performance of a finger-vein recognition system.

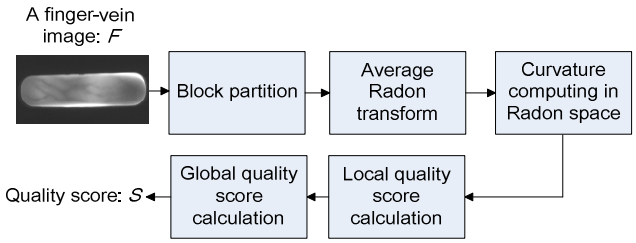

Fig. 2. The system flow diagram of the proposed finger-vein image quality assessment approach

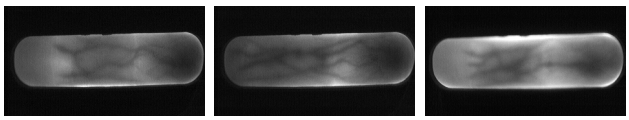

Fig. 3. Examples of high quality finger-vein images.

The organization of this paper is as follows: Section II introduces the proposed quality assessment approach for finger-vein images. Section III presents the experimental results, followed by the conclusions in the last section.

II. THE PROPOSED METHOD

Fig. 2. shows the system flow diagram of the proposed quality assessment approach. First of all, the given finger-vein image F is partitioned into a set of n non-overlapping blocks B_i with size $W \times H$, where i =1, 2, 3, ... , n, W and H refer to the width and height of the block, respectively. Then, each block is projected into Radon space using an average Radon transform. For a single block, the curvature in its Radon space is computed to measure the quality of the local vein patterns, from which a local quality score is estimated. Finally, the quality of the finger-vein image F is measured by a global quality score GS computed from all local quality scores.

A. Average Radon transform

The quality of a finger-vein image usually depends on the quantity and the contrast of the vein patterns. Fig. 3 shows three examples of high quality finger-vein images. Compared with the low quality finger-vein images shown in Fig. 1, these high quality finger-vein images contain more vein patterns with a higher contrast. Generally speaking, these vein patterns can be approximately treated as a combination of a set of line segments. Radon transform [8] is an effective tool to detect the line structures in the images. For each block B_i, the Radon Transform for a set of straight lines L is defined as follows:

$$\phi_i(\rho,\theta) = \iint_{(x,y)\in B_i} F(x,y)\delta[\rho-(x\cos(\theta)+y\sin(\theta))]dxdy \quad (1)$$

where δ is the Dirac delta function, ρ is the shortest distance from the center of block to L and θ refers to the angle of L. Fig. 4(a) shows the result of projecting a block into the Radon space using the Radon transform, where the angle of the straight lines L is the same as the main orientation of the vein pattern (denoted as θ_m where $0 < \theta_m \leq \pi$). It can be seen from Fig. 4(a) that the Radon transform can successfully detect the vein pattern which is close to the center o of the block due to the prominent valley in $\phi_i(\rho, \theta_m)$. However, for the vein pattern near the corner of the block, it may not be easily detected using the Radon transform. The reason is that the number of the pixels in the block are limited along L for such a vein pattern, which may not be able to create a prominent valley in $\phi_i(\rho, \theta_m)$.

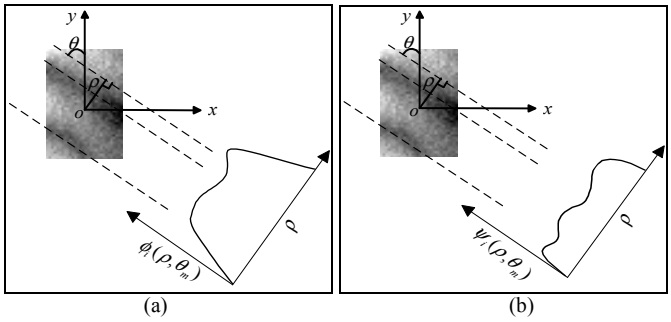

(a) (b)

Fig. 4. Projecting a block in the Radon space along the main vein direction θ_m (i.e., $\theta = \theta_m$) using (a) Radon transform and (b) average Radon transform. The dash lines refer to the straight lines L.

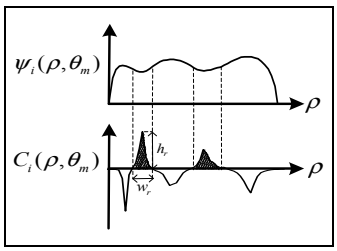

Fig. 5. Curvature in Radon space for the block shown in Fig. 4. The block is projected along the main orientation θ_m, the area in grid refers to the regions of valleys.

In order to extract all the vein patterns in each block. We propose to project each block into the Radon space by using an average Radon transform

$$\psi_i(\rho,\theta) = \frac{\psi_i(\rho,\theta)}{\Re} \quad (2)$$

where $\Re$ refers to the number of all the pixels in the block along L, i.e.,

$$\Re = \iint_{(x,y)\in B_i} \delta[\rho-(x\cos(\theta)+y\sin(\theta))]dxdy \quad (3)$$

Fig. 4(b) shows the results of projecting a block in the Radon space using the average Radon transform along the main vein orientation θ_m. We can see that there are prominent valleys in $\psi_i(\rho, \theta_m)$ for all the vein patterns in the block.

B. Curvature in Radon space

In order to distinguish the valleys in the Radon space, we

compute the curvature of the block B_i in Radon space, i.e.,

$$C_i(\rho,\ \theta)=\frac{d^2\psi_i(\rho,\theta)/d\rho^2}{\{1+(d\psi_i(\rho,\theta)/d\rho)^2\}^{3/2}} \tag{4}$$

Then, the region of valleys in the Radon space can be determined by $C_i(\rho,\ \theta)>0$ as illustrated in Fig. 5. To simplify the description of our approach in the following sections, the region of the rth valley in the Radon space is defined as $R_r(\rho_1,\ \rho_2,\ \theta)$, subject to

1) $\rho_2 > \rho_1$

2) $C_i(\rho,\ \theta) = 0$, if $\rho = \rho_1$ or ρ_2

3) $C_i(\rho,\ \theta) > 0$, if $\rho_1 < \rho < \rho_2$

For $R_r(\rho_1,\ \rho_2,\ \theta)$, we further define w_r and h_r as its width and height (see Fig. 5), where

$$w_r = \rho_1 - \rho_2 \tag{5}$$

and

$$h_r = max(C_i(\rho,\ \theta)) \tag{6}$$

where $\rho_1 < \rho < \rho_2$.

C. Local quality score estimation

In general, if the contrast of a vein pattern is high, the corresponding valley in $\psi_i(\rho,\theta_m)$ will be sharp with high curvature. Thus, the local quality score of each block can be estimated according to the curvature values of all the valleys in $\psi_i(\rho,\ \theta_m)$.

First of all, we have to find the main vein orientation θ_m for the block B_i. We quantize all the possible vein orientations into a set of K values as

$$\theta_q = \frac{q\pi}{K} \tag{7}$$

where $q = 1,\ 2,\ ...,\ K$ and K is heuristically set as 8. For the orientation θ_q, we project the block B_i into the Radon space $\psi_i(\rho,\ \theta_q)$ with the corresponding curvature $C_i(\rho,\ \theta_q)$. Suppose there are z regions of valleys $R_r(\rho_1,\ \rho_2,\ \theta_q)$ that can be determined from $C_i(\rho,\theta_q)$, we compute a temporary score for block B_i by

$$T_i(\theta_q)=\sum_{r=1}^{z}\frac{t_r(\theta_q)}{w_r} \tag{8}$$

where

$$t_r(\theta_q)=\begin{cases}\int_{\rho_1}^{\rho_2} C_i(\rho,\theta_q)d\rho & if\ \frac{h_r}{w_r}>\tau \\ 0 & otherwise\end{cases} \tag{9}$$

where τ is a threshold to determine whether $R_r(\rho_1,\rho_2,\theta_q)$ is prominent. For the regions of valley that are created due to the noise, the ratio h_r/w_r will usually be small. Such a region of valley will be considered as not prominent and ignored during the calculation of $T_i(\theta_q)$. After all the K temporary scores $T_i(\theta_q)$ are computed for B_i, the main vein orientation can be determined by

$$\theta_m = \underset{\theta_q}{\arg\max}\, T_i(\theta_q) \tag{10}$$

The local quality score of block B_i is estimated by

$$S_i = T_i(\theta_m) \tag{11}$$

D. Global quality score estimation

Based on the local quality score of each block, the global quality score of the finger vein image F can be computed by

$$GS = \frac{1}{n}\sum_{i=1}^{n} S_i \tag{12}$$

III. Experimental Results

To the best of our knowledge, there is no public finger-vein database. Therefore, we build a finger-vein database containing 8000 grayscale finger-vein images from 400 fingers with 20 different impressions per finger, where the size of each image is 311×171. The quality of each image is assessed by GS using our proposed quality assessment approach. We adopt a classical finger-vein recognition system [2] for extracting and matching the finger-vein features (i.e., the binary finger-vein images) from the finger-vein images. In the experiments, the width and height of a block are 20 and 40, respectively. τ is set to 0.06 heuristically.

A. The performance evaluation

We identify a finger-vein image as a low quality image if its quality score GS is less than a certain threshold. Following steps are performed to evaluate the accuracy of our quality assessment approach for identifying the low quality finger-vein images.

1) Selection of the template:

We select one finger-vein image with the highest quality by human vision among the 20 impressions for each finger, which is the enrolled template stored in a database. The other 19 impressions are testing finger-vein images during the experiment. In total, there are 400 enrolled templates and 7600 (400 × 19) testing images.

2) Matching the finger-vein images:

In order to compute the False Rejection Rate (FRR), each enrolled template is matched against the corresponding testing finger-vein images, producing 400 × 19=7600 genuine tests. In order to compute the False Acceptance Rate (FAR), each enrolled template is matched against the other 399 templates, producing 400×399/2=79800 impostor tests, where the symmetric imposter tests are not performed.

3) Computing the accuracy for identifying the low quality finger-vein images:

Among all the 7600 testing finger-vein images, we denote α as the number of the identified low quality images. Among

all α identified low quality images, we further denote β as number of the images that are falsely rejected by the system at a certain FAR. The accuracy for identifying the low quality finger-vein images is computed by

$$\eta = \frac{\beta}{\alpha} \tag{13}$$

We set five different levels of threshold for the proposed approach. Table I gives the number of the low quality images identified at different levels. At level 1, for example, the 200 images with the lowest 200 scores among all the testing images are identified as low quality images.

TABLE I. NUMBER OF THE IDENTIFIED LOW QUALITY IMAGES (A) AT DIFFERENT LEVELS OF THRESHOLD

	Level of threshold				
	1	2	3	4	5
α	200	500	800	1100	1400

Table II lists the accuracy η for identifying the low quality images at different levels and FAR. It can be seen that the proposed approach can effectively identify the low quality finger-vein images. For the proposed approach at level 1 and FAR= 0.01%, 93.50% of the low quality images identified are actually rejected by the finger-vein recognition system. When the level increases, more finger-vein images will be identified as low quality images (see Table II) but the accuracy η reduces. On the other hand, when FAR increases, there are fewer finger-vein images that are falsely rejected by the system, which will also create a reduction in η at the same level.

TABLE II. THE ACCURACY FOR IDENTIFYING THE LOW QUALITY FINGER-VEIN IMAGES (THE ENROLLED TEMPLATES ARE SELECTED MANUALLY)

		η(%)				
level		1	2	3	4	5
FAR	0.01%	93.50	85.60	82.63.	78.45	75.43
	0.10%	88.50	75.80	70.37	64.36	60.57

B. *Effects on the finger-vein recognition system*

In this section, we examine how the performance of the finger-vein recognition system [2] would be affected by adopting our quality assessment approach. Specifically, we calculate the Equal Error Rate (EER) of the system before and after filtering the identified low quality images (using our approach) among the 19 testing finger-vein images of each finger.

TABLE III. THE EER OF THE FINGER-VEIN RECOGNITION SYSTEM AFTER FILTERING THE LOW QUALITY FINGER-VEIN IMAGES USING OUR APPROACH

	EER(%)				
level	1	2	3	4	5
Manual	6.27	5.87	5.35	5.23	5.00

Before the filtering, there are 400×19 = 7600 genuine tests and 400 ×399/2 = 79800 impostor tests, which are the same as the step 2) described in Section III-A. When the templates are manually selected, the EER of the finger-vein recognition system is 7.01%. During the filtering, we do not consider the genuine tests performed from the low quality testing images and the corresponding templates. Table III lists the EER of the finger-vein recognition system after filtering the low quality testing images using the proposed approach at different levels, where Manual refer to the case when the templates are manually selected. It can be seen that the EER of the system reduces after filtering. By using the proposed approach at level 5, the EER of the system reduces to 5.00%.

IV. CONCLUSION

A novel quality assessment approach for finger-vein image is proposed in this paper. The quality of a finger-vein image is estimated based on the local quality of different blocks. In order to measure the local quality, each block is projected into the Radon space using an average Radon transform. A local quality score is estimated for each block according to the curvature in its Radon space, based on which a global quality score is computed for the finger-vein image. The experimental results show that our proposed approach works well for identifying the low quality finger-vein images, and the EER of a finger-vein recognition system can be reduced by incorporating our quality assessment approach for filtering the low quality testing finger-vein images. In addition, an extended version by considering the quality of the binary version of the finger-vein image is expected to achieve better performance[1].

REFERENCES

[1] A. Kumar and Y. Zhou, "Human identification using finger images," *IEEE Transactions on Image Processing*, vol. 21, no. 4, pp. 2228 –2244, 2012.

[2] N. Miura, A. Nagasaka, and T. Miyatake, "Extraction of finger-vein patterns using maximum curvature points in image profiles," *IEICE Transactions on Information and Systems*, vol. E90D, no. 8, pp. 1185–1194, Aug. 2007.

[3] B. Huang, Y. Dai, R. Li, D. Tang, and W. Li, "Finger-vein authentication based on wide line detector and pattern normalization," *in Pattern Recognition (ICPR),* 2010 20th International Conference on, Aug. 2010.

[4] Y. Zhou and A. Kumar, "Human identification using palm-vein images," *IEEE Transactions on Information Forensics and Security*, vol. 6, no. 4, pp. 1259 –1274, 2011.

[5] L. Shen, A. Kot, and W. Koo, "Quality measures of fingerprint images," *in Audio Video-Based Person Authentication*, vol. 2091, 2001, pp. 266–271..

[6] M. Abdel-Mottaleb and M. Mahoor, "Application notes - algorithms for assessing the quality of facial images," *IEEE Computational Intelligence Magazine*, vol. 2, no. 2, pp. 10 –17, 2007.

[7] C. Belcher and Y. Du, "A selective feature information approach for iris image-quality measure," *IEEE Transactions on Information Forensics and Security*, vol. 3, no. 3, pp. 572 –577, 2008.

[8] S. R. Deans, The Radon transform and some of its applications. *Krieger Publishing Company*, 1983.

[1] An extended version of the paper has been submitted to IEEE Transactions on Information Forensics and Security.